◎ 논 문
◎ Original Paper

DOI: http://dx.doi.org/10.5293/kfma.2019.22.6.005
ISSN (Print): 2287-9706

J-Groove를 이용한 펌프터빈 흡출관 유동 불안정성 억제

쉬레스트 우즈왈* · 패트릭 마크 싱** · 최영도***†

Suppression of flow instability in draft tube of Pump Turbine using J-Groove

Ujjwal Shrestha*, Patrick Mark Singh**, Young Do Choi***†

Key Words : Pump-Turbine(펌프터빈), Performance(성능), Draft Tube(흡출관), Swirl Flow(선회류), J-Groove(J-그루브)

ABSTRACT

In the present study, J-Groove has applied in the diffuser for swirl intensity suppression. The swirl flow mostly occurred at the draft tube of the hydro turbine. The swirl flow is an undesirable flow phenomenon, which is a cause of pressure fluctuation, mechanical vibration, and noise. The performance analysis of the pump turbine was conducted by experiment and CFD analysis. In the pump turbine, the swirl flow is significant in the turbine mode rather than pump mode. The swirl intensity is high at partial load conditions. Pump-turbine performance has deteriorated in off-design conditions due to the high swirl intensity. The J-Groove installation helps to decrease the swirl intensity at the partial load condition without affecting the performance of the pump turbine.

1. Introduction

The operating range of the hydro pump turbine has limited because it requires to perform well in turbine mode as well as pump mode. Flow stability is a concern for the better performance of pump-turbine. When pump turbine operates in partial load condition, the swirl intensity rises in the draft tube that leads to the higher pressure fluctuation. The abnormalities like noise, vibration, and performance degradation are accompanied by the higher pressure fluctuation[1].

Several papers have discussed the numerical and experimental analysis to predict the vortex rope in the draft tube. Nicolet et al.[2] conducted an investigation of the Francis turbine vortex rope at the upper part load condition by experiments. The vortex rope has been detected with the help of flow visualization. The frequency of pressure fluctuation in the draft tube in a range of 1 to 3 times of runner rotational frequency (f_n) was found in high specific speed Francis turbine. Rodriguez et al.[3] studied high load vortex oscillations developed in a Francis hydro turbine.

The vortex rope in the draft tube is very unpleasant for the hydro turbine performance. Myriad techniques have implemented for the alleviation of pressure fluctuation from the draft tube of Francis hydro turbine Air supplied just below the runner at the draft tube inlet is an efficient method to depress the pressure fluctuation[4-8].

The unsteady flow in the turbo-machines can be effectively alleviated by the application of J-Groove[9]. 'J' means the 'Jet' flow occurring in the groove channel, which counteracts the centrifugal forces in the vortex rope that is formed in the flow passage. There is jet

* Graduate School, Department of Mechanical Engineering, Mokpo National University
** Department of Mechanical Engineering, Fiji National University
*** Department of Mechanical Engineering, Institute of New and Renewable Energy Technology Research, Mokpo National University
† 교신저자, E-mail : ydchoi@mokpo.ac.kr

The KSFM Journal of Fluid Machinery: Vol. 22, No. 6, December 2019, pp.05~13(Received 21 Dec. 2018; revised 18 Oct. 2019; accepted for publication 18 Nov. 2019)
한국유체기계학회 논문집: 제22권, 제6호, pp.05~13, 2019(논문접수일자: 2018.12.21, 논문수정일자: 2019.10.18, 심사완료일자: 2019.11.18)

flow in the groove because of the intense pressure gradient, which runs from the high-pressure region to low pressure region. Choi et al.[10] have implemented the J-Groove on the inducer and conical shape diffuser for the suppression of the cavitation. Kurokawa et al.[11] have investigated the influence of J-Groove installation on swirl flow suppression in the conical shape diffuser. Wei et al. have been conducted various studies on the application of J-Groove in the draft tube of a Francis hydro turbine[12,13]. Moreover, the implementation of the J-Groove in the draft tube of Francis hydro turbine is effective for the reduction of swirl intensity and pressure fluctuation[14].

However, there are not many studies regarding J-Groove employment in pump turbines. In this study, the J-Groove is installed in the draft tube of the pump turbine, and its influences on swirl intensity and pressure fluctuation are investigated.

2. Experimental and Numerical Methods

2.1 Pump turbine test model

The meridional shape of the pump turbine is indicated in Fig. 1. The flow direction in the meridional shape represents the pump mode. The design of the pump turbine is based on a gradient of discharge variation to the head variation method[15].

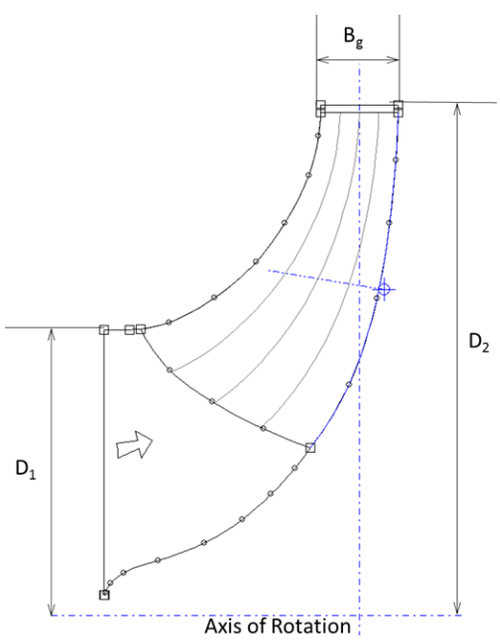

Fig. 1 Meridional shape of pump turbine

The detailed design specification of the pump turbine model is shown in Table 1. Considering the pump mode, the inlet and outlet diameter of pump-turbine are D_1=112 mm and D_2=198 mm respectively. The pump turbine size, which is indicated above, refer to pico hydro size. The number of the impeller for the pump turbine is Z_r=5. Additionally, the number of stay vanes and guide vanes are Z_g=14 and Z_s=14, respectively. The operating condition of the pump turbine model is slightly different in turbine mode and pump mode. The turbine mode operates on the head, H=15 m, flow rate, Q=0.026 m^3/s, and rotational speed, N=1800 min^{-1}. For the pump mode, it operates on the head, H=16.5 m, flow rate, Q=0.020 m^3/s, and rotational speed, N=1800 min^{-1}. The performance validation of the pump turbine has been conducted using the experiment facility shown in Fig. 2.

Table 1 Specification of Pump Turbine

Specification	Turbine	Pump
Head (m)	15.0	16.5
Flow Rate (m^3/s)	0.026	0.020
Specific Speed	95 m-kW	31 m-m^3/s
Rotational Speed (min^{-1})	1800	
D_1 (mm)	112.0	
D_2 (mm)	198.0	
B_g (mm)	15.2	
Number of Blades, Z_r	5	
Number of Guide Vanes, Z_g	14	
Number of Stay Vanes, Z_s	14	
Speed factor, $\frac{2\pi N D_2}{60(gH)^{0.5}}$	3.077	2.933
Discharge factor, $\frac{Q}{D_2^2(gH)^{0.5}}$	0.055	0.040
Power factor, $\frac{P}{\rho D_2^2(gH)^{1.5}}$	0.043	0.037

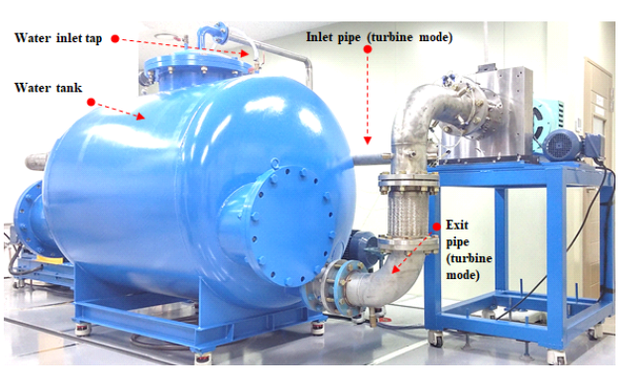

Fig. 2 Experimental test facility for pump turbine

2.2 J-Groove Model

According to Saha[16,17], it has been known that the design of the J-Groove mainly affected by its length (l_z), depth (y), angle (θ), and number (n). Fig. 3 shows the design parameter of J-Groove. Fig. 4 shows the fluid domain of diffuser with J-Groove installation in its wall. The length, depth, angle, and number are l_z=120 mm, y=4 mm, θ=15° , and n=12, respectively. The J-Grooves are uniformly distributed throughout the circumference of the diffuser.

2.3 Numerical Method

The fluid domain of the pump-turbine geometry was modeled in 3D. The numerical mesh was generated using ANSYS ICEM 18.1, and the analysis and calculation were conducted using a commercial software ANSYS CFX 18.1[18].

The numerical mesh for all the components was constructed using the hexahedral mesh. The full domain calculation model and the refined hexahedral mesh are shown in Fig. 5. An acceptable y+ value is below 30 in all domains. Mesh size of 5.65×106 nodes was selected for CFD analysis of the pump turbine from the mesh independency test indicated in Fig. 6. Mesh independency test provides an optimum mesh number to reduce computation time and an acceptable y+ value of 26.76 for a runner. The y+ values for the other components were below 30. The y+ value for the draft tube is 8.9.

The numerical analysis has been carried out with boundary conditions summarized in Table 2. The connection between the rotational interface and fixed interfaces was set as a frozen rotor for a steady state

Table 2 Boundary conditions for numerical method

Specification	Turbine	Pump
Inlet	Total Pressure	Static Pressure
Outlet	Static Pressure	Mass Flow Rate
Turbulence Model	Shear Stress Transport	
Interface Model	Steady: Frozen Rotor	
	Unsteady: Transient Rotor Stator	
Time Step	Unsteady: 9.25×10^{-5} sec	
Reference Pressure	1 atm	
Wall Condition	No Slip Wall	

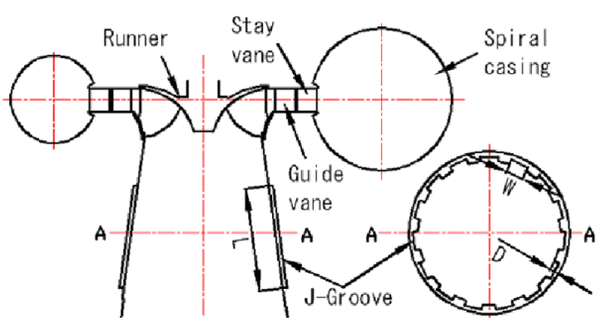

Fig. 3 Pump turbine cross section view

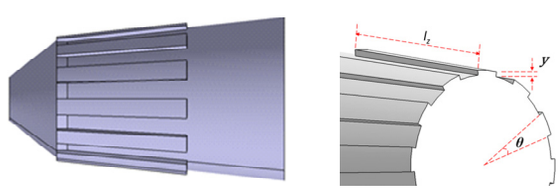

Fig. 4 3D view of J-Groove and its parameter

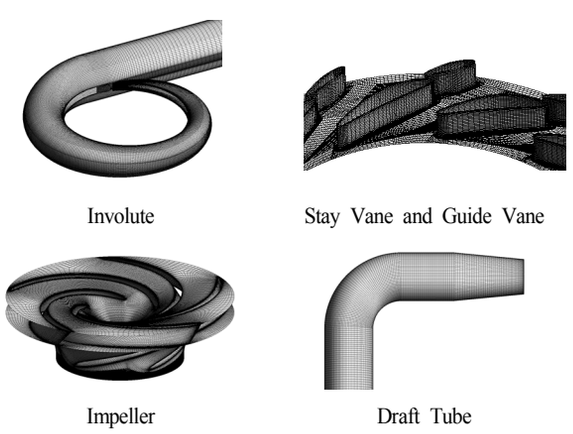

Fig. 5 Numerical mesh for fluid domain of pump turbine

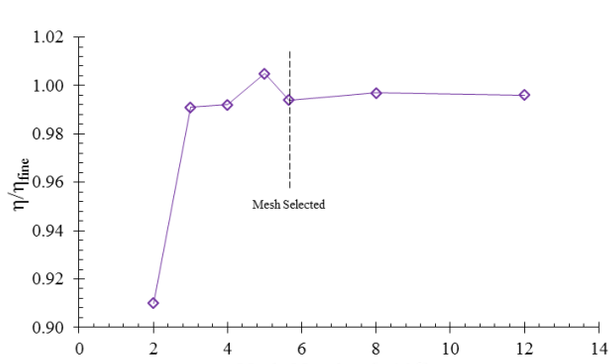

Fig. 6 Mesh Independence test for pump turbine model

calculation and transient rotor–stator for unsteady calculation. Shear Stress Transport (SST) turbulence model was used for the CFD analysis. SST can estimate both separation and vortex occurrence on the wall of complex blade shapes.

In turbine mode, the total pressure and static pressure are applied at inlet and outlet respectively. With this boundary condition, the head can be fixed while the flow rate is determined by calculation according to different guide vane opening. In the pump mode, the static pressure and mass flow rate are applied at inlet and outlet, respectively. The frozen rotor is selected as an interface model from the previous study[15].

3. Results and Discussion

3.1 Performance of the pump–turbine model

The performance characteristics of the pump turbine are presented in Fig. 7. The results of both pump and turbine modes have been included providing the efficiency, power, and head according to the unit flow rate, Q_{11}.

It is difficult to match the boundary conditions of experimental and numerical analysis. Therefore, the results between experimental and numerical analyses have been compared to the unit flow rate. CFD analysis results are recalculated by using experimental boundary conditions. From Fig. 7, it is obvious that the results of the experimental analysis match well with the results of CFD analysis. The deviation between experimental and CFD analysis results is in the acceptable range. Therefore, the CFD analysis results are reliable for the prediction of the internal flow of the pump turbine.

The maximum efficiencies by experiment in turbine mode and pump mode were achieved as 84.1% and 84.9%, respectively. The best efficiency point occurs at Q_{BEP} = 0.165 for turbine mode and Q_{BEP} = 0.125 for pump mode.

The head loss by CFD analysis for turbine mode and pump mode at the best efficiency point is illustrated in Fig. 8. The head loss has represented by the percentage of efficiency loss in the pump turbine. The loss analysis of the pump–turbine model indicates that losses in the stay vane and guide vane are slightly more than that of the impeller in pump mode. However, the loss in impeller in turbine mode is higher than that at pump mode. From the loss analysis, it can be inferred that loss is high at the outlet of an impeller in both modes. This indicates that the flow from the impeller is unstable. The flow coming out from the impeller has a high amount of swirl and non–uniform distribution.

3.2 Effect of J–Groove on Performance

The effect of J–Groove has been investigated by experimental analysis. The performance curves by the experimental results are compared for the pump and

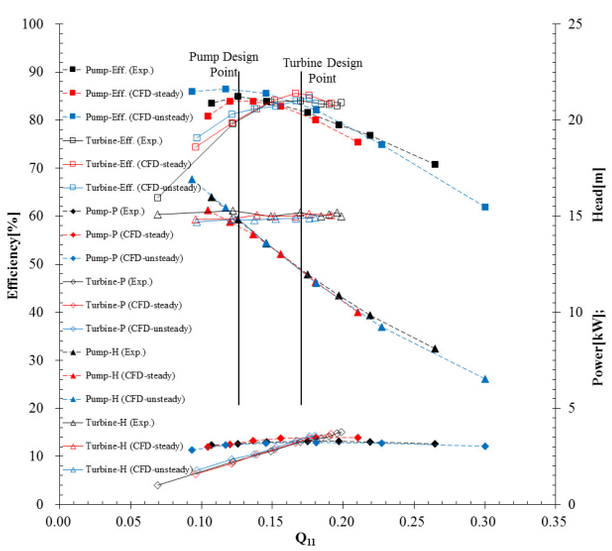

Fig. 7 Pump turbine performance characteristics comparison of experiment and CFD analysis (without J–Groove)

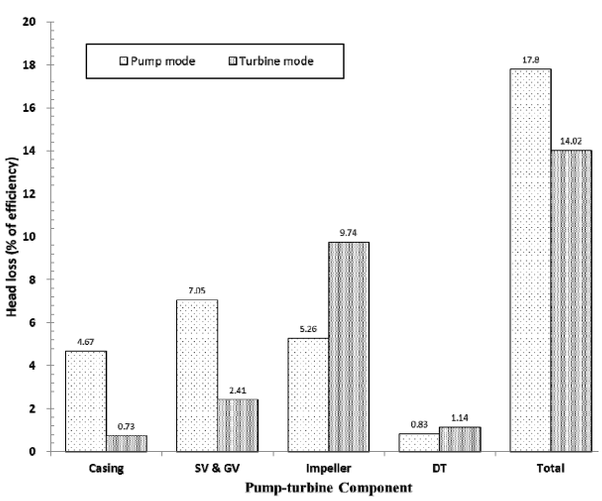

Fig. 8 Loss analysis as percentage of efficiency at BEP for both modes (without J–Groove)

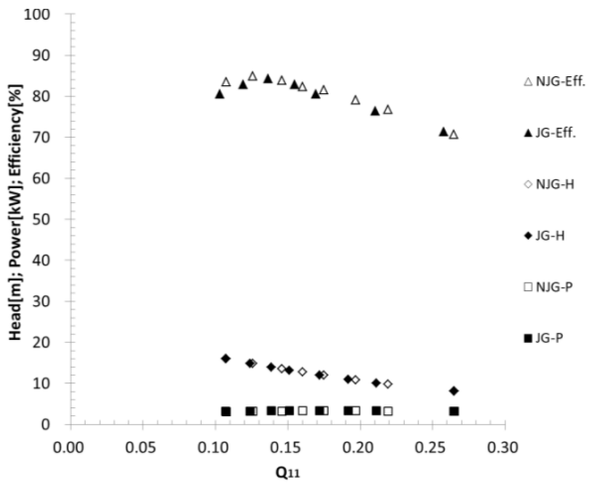

Fig. 9 Comparison of pump turbine performance with and without J-Groove in pump mode by experiment

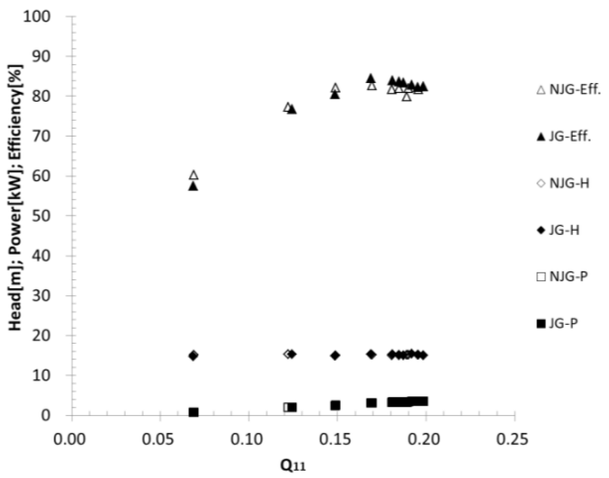

Fig. 10 Comparison of pump turbine performance with and without J-Groove in turbine mode by experiment

turbine modes at normal operating conditions in Figs. 9 and 10. The two results show slightly contradicting trends when the J-Groove is applied. In Figs. 9 and 10, NJG and JG represent the draft tube without J-Groove and draft tube with J-Groove.

However, J-Groove installation shows a positive effect on the turbine while operating in the best efficiency point. The J-Groove installation makes a slight drop in efficiency while operating in a partial flow rate. The power generation and consumption are not influenced by J-Groove installation.

In pump mode, J-Groove installation shows both rise and drop in the efficiency, which is shown in Fig. 9. The efficiency has been drop when pump mode required a higher flow rate and vice versa. However, in the turbine mode, the efficiency drops by 0.4 % at a low flow rate, and no significant change is observed at a high flow rate. The installation of J-Groove has no significant effect on the pump turbine efficiency in both modes.

3.3 Swirl Intensity Distribution

The swirl intensity distribution is an effective method to estimate the J-Groove effect. Equation 1 shows the relation of swirl intensity, S_n with axial velocity, V_z and circumferential velocity, V_θ. The numerator indicates the axial flux of tangential momentum. The denominator indicates the axial thrust [19,20].

$$S_n = \frac{\int_0^r V_z V_\theta r^2 dr}{R\int_0^r V_z^2 r dr} \quad (1)$$

where, r = radial position

R = draft tube cross section radius

Swirl intensity distribution has been measured in different cross-sections of the draft tube as illustrated in Fig. 11. The pressure distribution with and without J-Groove has shown in Fig. 12. It is clear from Fig. 12 that the pressure is increased in the draft tube with the installation of J-Groove. Fig. 13 shows the behavior of swirl intensity distribution with a change in flow rate in turbine mode. The flow rate and swirl intensity are inversely related to each other. The variation of swirl intensity distribution causes pressure fluctuation, vibration, and cavitation next to the impeller outlet.

The increase in swirl intensity refers that at a particular location the tangential thrust is more than the axial thrust, and thus, the loss in draft tube uprise. Figs. 14 and 15 show the effect of J-Groove in the suppression of swirl flow at different operating conditions. The swirl intensity distribution is significant in partial flow conditions. In partial flow rate Q/Q_{BEP} = 0.7, the J-Groove shows significant reduction in the swirl intensity throughout the draft tube. There is a slight reduction in the swirl intensity while operating at Q/Q_{BEP} =1. The J-Groove influence

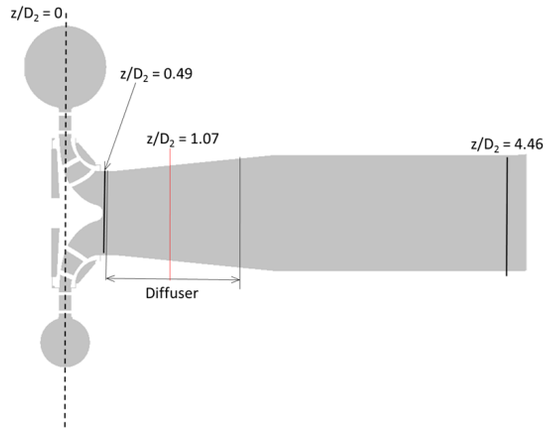

Fig. 11 Measuring location for swirl intensity and tangential velocity (red line)

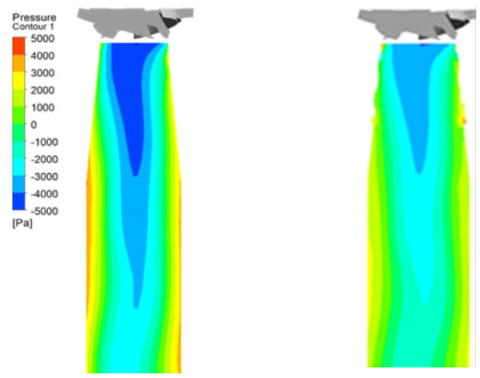

Fig. 12 Pressure distribution at draft tube a) without J-Groove b) with J-Groove

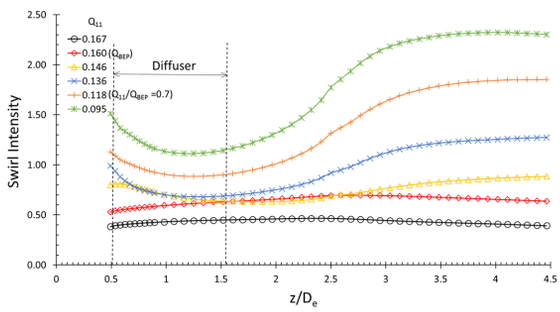

Fig. 13 Swirl intensity distribution without J-Groove in turbine mode by CFD analysis

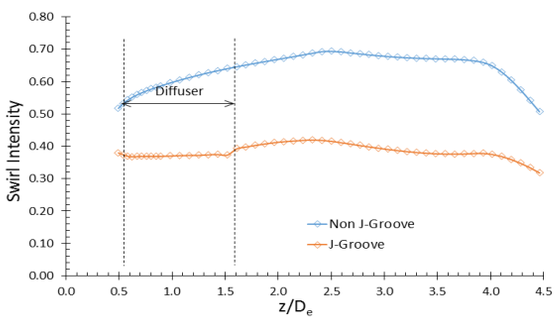

Fig. 14 Swirl intensity distribution at Q/Q_{BEP} =1 in turbine mode by CFD analysis

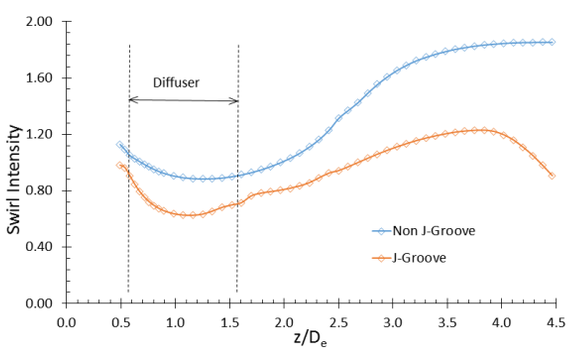

Fig. 15 Swirl intensity distribution at Q/Q_{BEP} = 0.7 in turbine mode by CFD analysis

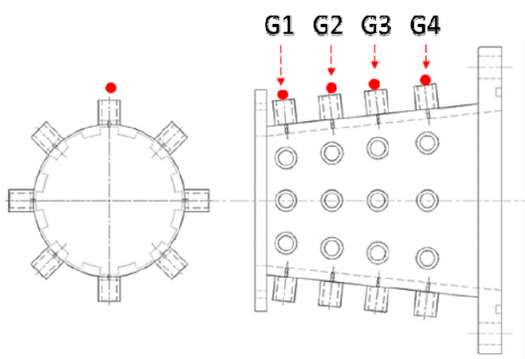

Fig. 16 Pressure data acquisition points in diffuser

is not limited within the diffuser, but throughout the draft tube.

3.4 Pressure Fluctuation Distribution

The monitoring points G1, G2, G3, and G4 are selected to evaluate pressure during experiment. The monitoring points are shown in Fig. 16.

Fast Fourier transformations have been implemented for the analysis of pressure fluctuations in the draft tube of pump turbine with and without J-Groove. From the FFT analysis, the peak pressure amplitude has occurred at the frequency in the range of 1-3 times of runner rotational frequency, f_n. Figs. 17-20 illustrate the pressure fluctuation analysis at the various location of the draft tube. When the flow is moving along the draft tube, J-groove installation suppresses the pressure fluctuation in the draft tube.

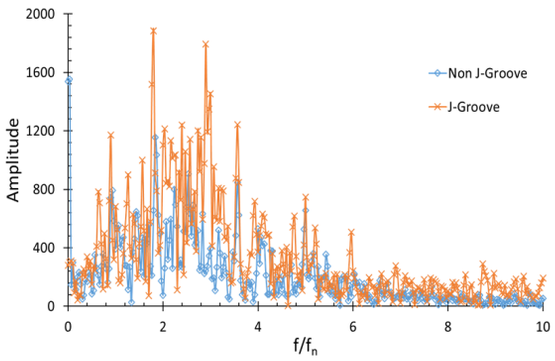

Fig. 17 Pressure fluctuation at G1 in turbine mode by experiment (Q/Q_{BEP} =0.6)

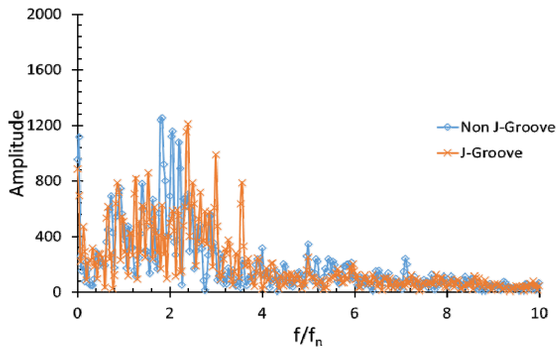

Fig. 18 Pressure fluctuation at G2 in turbine mode by experiment (Q/Q_{BEP} =0.6)

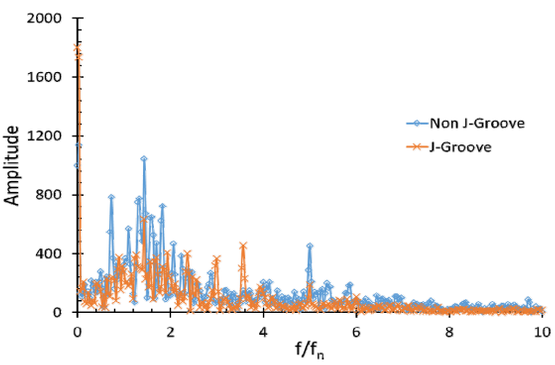

Fig. 19 Pressure fluctuation at G3 in turbine mode by experiment (Q/Q_{BEP} =0.6)

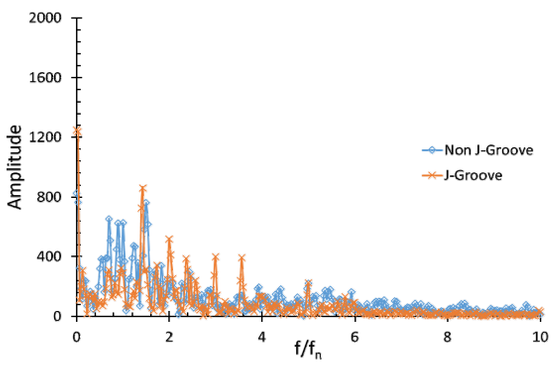

Fig. 20 Pressure fluctuation at G4 in turbine mode by experiment (Q/Q_{BEP} =0.6)

Fig. 17 indicates that the peak pressure fluctuation occurs at the frequency of 1 to 3 times of runner rotational frequency. At the outlet of the runner, the pressure fluctuation with J-Groove is high, which implies that the vortex core is stronger. Figs. 18-20 shows the suppression of pressure fluctuation in the draft tube with the installation of J-Groove. This implies that when flow passes from the J-Groove, the strength of the vortex core decreases drastically.

Fig. 21 indicates the vortex rope in the draft tube without and with J-Groove. The vortex rope has been created with the absolute static pressure of 96325 Pa. The strength of the vortex rope in the draft tube without J-Groove is much stronger than the draft tube with J-Groove. The length of the vortex rope is suppressed with the installation of J-Groove in the draft tube. The pressure fluctuation at the outlet of the runner is high because of the stronger vortex rope.

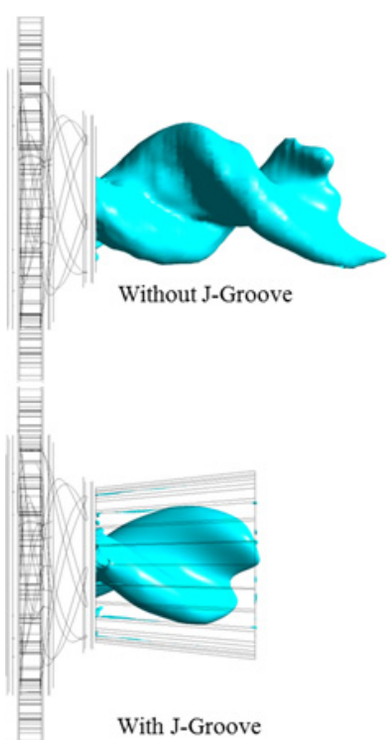

Fig. 21 Vortex rope visualization in draft tube without and with J-Groove by CFD analysis (Q/Q_{BEP} =0.6, t =0.213 s)

Fig. 11 indicates the velocity measuring location in the draft tube of the pump turbine in turbine mode. According to the velocity triangle shown in Fig. 22, the tangential component of the velocity should absent for ideal flow conditions. However, the complete removal of the tangential component is impossible. Fig. 23 shows the comparison of the tangential velocity without and with J-Groove installation. The installation of J-Groove has successfully suppressed the tangential velocity. The decrease in the tangential component of the velocity helps to suppress the recirculation flow in the draft tube. Therefore, the installation of the J-Groove makes minimum recirculation flow in the draft tube.

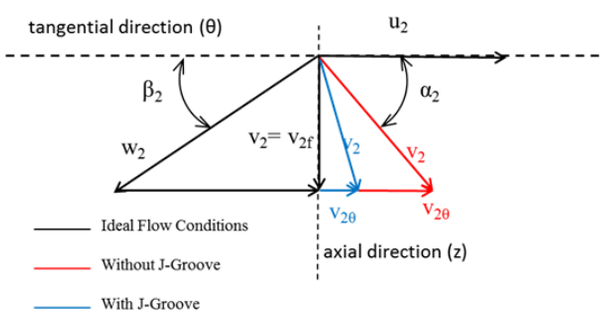

Fig. 22 Velocity triangle at measuring location

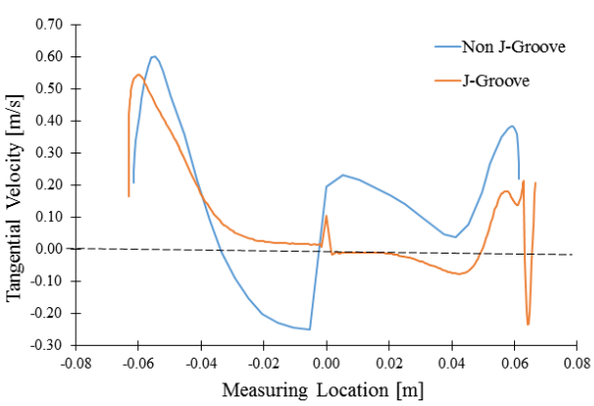

Fig. 23 Tangential velocity distribution at measuring location in turbine mode (Q/Q_{BEP} =0.6)

4. Conclusion

In this study, the effect of J-Groove installation on the performance of the pump turbine in the turbine mode and pump mode has investigated by experiment. The performance of the pump turbine is not affected by the installation of J-Groove. The loss analysis of the pump turbine indicates that pump mode has more head loss compare to turbine mode. In pump mode, stationary components like stay vane and guide vane have a significant contribution to the loss.

While operating in partial load conditions, the swirl flow in the draft tube is very high. The high swirl flow is undesirable for the smooth operation of the pump turbine. With the installation of J-Groove in the diffuser, the swirl intensity in the draft tube has been decreased significantly at partial load conditions. While operating in the best efficiency point, J-Groove has minimal influence on the suppression of swirl intensity. The pressure at the different location of the diffuser has been obtained from the experiment. The amplitude of the pressure fluctuation has minimized with the J-Groove installation in the diffuser.

In this study, the effectiveness of J-Groove on the pump turbine model has been verified. The implementation of J-Groove in real scale pump turbine is possible by applying hydraulic similitude. According to IEC 60193, the equality of speed factor, discharge factor and power factors characterize the hydraulic similitude of both pump turbine model and prototype. Therefore, the influence of J-Groove on model and prototype will be similar.

Acknowledgement

This research was supported by research funds of Mokpo National University in 2018.

References

(1) Biname, M., Su, W-T., Li, X-B., Li, F-G., Wei, X-Z., and An, S., (2017), "Investigation on pump as turbine (PAT) technical aspects for micro hydropower schemes: A state-of-the srt review", Renewable and Sustainable Energy Reviews, 79, pp. 148-179.

(2) Nicolet, C., Zobeiri, A., Maruzewski, M., and Avellan, F., (2010), "On the Upper Part Load Vortex Rope in Francis Turbine: Experimental Investigation", IOP Conference Series: Earth and Environmental Science, 12(1), 012053.

(3) Rodriguez, D., Rivetti, A., and Lucino, C., (2016), "High Load Vortex Oscillations Developed in Francis Turbines", IOP Conference Series: Earth and Environmental Science, 49(8) 082006.

(4) Qian, Z-D., Yang, J-D., and Huai, W-X., (2007), "Numerical Simulation and Analysis of Pressure Pulsation

in Francis Hydraulic Turbine with Air Admission", Journal of Hydrodynamics, Ser. B, 18 (4), pp. 467-472.
(5) Papillon, B., Sabourin, M., Couston, M., and Deschenes, C., (2002), "Methods for Air Admission in Hydroturbines", Proc. of the 21st IAHR Symposium on Hydraulic Machinery and Systems, Lausanne .
(6) Huang, R., An, Y., Luo, X., and Ji, B., (2014), "Numerical Simulation of Pressure Vibrations in a Francis Turbine Draft Tube with Air Admission", Proc. of the ASME 2014 4th Joint US-European Fluids Engineering Division Summer, Chicago, Illinois, USA.
(7) Yu, A., Luo, X. W., and Ji, B., (2015), "Numerical Simulation and Analysis of the Internal Flow in a Francis Turbine with Air Admission", IOP Conf. Series: Materials Science and Engineering, 72(4) 042047.
(8) Li, W. F., Feng, J. J., Wu, H., Lu, J. L., and Luo, X. Q., (2015), "Numerical Investigation of Pressure Fluctuation Reducing in Draft Tube of Francis Turbines", International Journal of Fluid Machinery and Systems, 8(3) pp. 202-208.
(9) Kurokawa, J., (2011), "J-groove technique for suppressing various anomalous flow phenomena in turbomachines", International Journal of Fluid Machinery and Systems, 4(1), pp. 1-13.
(10) Choi, Y-D., Kurokawa, J., and Imamura, H., (2007), "Suppression of Cavitation in Inducers by J-Grooves", Journal of Fluids Engineering (ASME), 129,(1), pp. 15-22.
(11) Kurokawa, J., Imaumura, H., and Choi, Y-D., (2010), "Effect of J-groove on the suppression of swirl flow in a conical diffuser", Journal of Fluids Engineering, 132, 071101.
(12) Wei, Q., Zhu, B., and Choi, Y-D., (2012), "Internal Flow Characteristics in the Draft Tube of a Francis Turbine", Journal of the Korean Society of Marine Engineering, 36(5), pp. 618-626.
(13) Wei, Q., (2012), "Suppression of Abnormal Phenomena in the Draft Tube of a Francis Hydro Turbine Model by J-Groove", Master Thesis, Mokpo National University.
(14) Chen, Z., Singh, P. M., and Choi, Y-D., (2017), "Suppression of unsteady swirl flow in the draft tube of a Francis hydro turbine model using J-Groove", Journal of Mechanical Science and Technology, 31(12), pp. 5813-5820.
(15) Singh, P. M., Chen, Z. and Choi, Y. D., 2017, "Hydraulic design and performance analysis on a small pump turbine system for ocean renewable energy storage system," Journal of Mechanical Science and Technology, 31(11), pp. 5089-5097
(16) Saha, S. L., Kurokawa, J., Matsui, J., and Imamura, H., (2000), "Suppression of performance curve instabiligy of a mixed flow pump by use of J-groove", Journal of Fluids Engineering, 122, pp. 592-597.
(17) Saha, S. L., Kurokawa, J., Matsui, J., and Imamura, H., (2001), "Passive control of rotating stall in aparallel-wall vaned diffuser by J-Grooves", Journal of Fluids Engineering, 123(1), pp. 507-515.
(18) ANSYS Inc., "ANSYS CFX documentation ver. 18.1", http://www.ansys.com.(2017)
(19) Susan-Resiga, R. F., Muntean, S., Avellan, F., and Anton, I., (2011), "Mathematical modelling of swirling flow in hydraulic turbines for the full operating range", Applied Mathematical Modelling, 35, pp. 4759-73.
(20) Saqr, K. M., and Wahid, M. A., "Effects of swirl intensity on heat transfer and entropy generation in turbulent decaying swirl flow", Applied Thermal Engineering, 70, pp. 468-49.